PHYSICAL REVIEW C VOLUME 24, NUMBER 4 OCTOBER 1981

Molecular resonance effects in heavy ion excitation functions

S. Y. Lee, Y. H. Chu, and T. T. S. Kuo
Department of Physics, State University of New York at Stony Brook, Stony Brook, New York 11794
(Received 22 May 1980)

The inelastic and fusion excitation functions are analyzed using an interference mechanism between the barrier and internal waves of the heavy ion optical potential. The undamped overlapping molecular resonances are found to be the main dynamical mechanism for the gross oscillations in the excitation function. Our result suggests a rather interesting correlation between the total reaction excitation and the direct surface reaction excitation function. Its origin may be understood as follows: At the resonance, the wave function is pulled into the nuclear interior, and thus, the total reaction cross section is at maximum. The direct surface reaction is, however, shifted by a small phase difference near the surface region. This picture should be valid in the case of overlapping molecular resonance of the heavy ion systems. Good agreement between calculated and experimental inelastic and fusion excitation functions for $^{12}C+^{12}C$ and $^{16}O+^{16}O$ is obtained.

[NUCLEAR REACTIONS Effect of molecular resonance to the gross oscillation in heavy ion inelastic and fusion excitation functions.]

I. INTRODUCTION

Recently, Phillips *et al.*[1] proposed an interesting explanation of the $^{12}C+^{12}C$ and $^{16}O+^{16}O$ low lying state inelastic excitation functions.[2] For these systems of inelastic heavy ion scattering, the angle integrated cross sections exhibit gross oscillations as well as fine structures. Phillips *et al.*[1] pointed out that the essential ingredient of these gross oscillations is due to the kinematic matching condition for the initial and final channels. Since the direct inelastic scattering is a surface reaction, the grazing angular momenta of the initial and final channels play an important role in the reaction mechansim. The reaction is considered to proceed via two angular momentum windows around the grazing angular momenta of the entrance and exit channels. However, this simple interesting picture has a rather serious drawback in that the angular momentum window required in this diffraction model is too small to be consistent with that calculated from the heavy ion proximity potential.[3] Friedman *et al.*[4] reinterpreted the work of Phillips *et al.* as the kinematic matching condition of the barrier top resonances[5] of the initial and final channels. Since the physics of the "barrier top resonance" is by and large equivalent to the physics of the grazing angular momentum phenomena, we do not distinguish between these two interpretations.

Alternatively, these data have also been analyzed by the band-crossing model,[6] where a set of rotational bands has been assumed to couple strongly to the entrance and exit channels. Then, an l or J-independent absorption[7] is used to simulate the isolated resonances in the entrance and exit channels. The band crossing model is also quite successful in fitting these oscillations with a number of free parameters. It is not clear, however, what the essential ingredient is of the physics behind this picture. The model relies essentially on a very weak absorption around the grazing angular momentum. The physics of the l or J-dependent absorption is interesting, yet it demands more experimental justification.

In this paper, we present a new explanation of these observed gross oscillations in the inelastic $^{12}C+^{12}C$ and $^{16}O+^{16}O$ excitation functions. Our analysis is based on the interference mechanism[8] between the barrier wave and the internal wave amplitudes. We shall try to use as few free parameters as possible. To this end, the Austern-Blair (AB) model[9] of the distorted wave Born approximation (DWBA) will be used in our study. This

should be a fairly accurate approximation for the low lying states of nuclei near the spherical region with moderate absorption. The interference mechanism between the barrier and the internal waves has been observed in the elastic scattering of many heavy ion systems. However, it has not yet been applied to the inelastic scattering. Our subject is to study the essential physics of the gross oscillation in the inelastic exictation function within the general framework of the interference mechanism. The proximity potential[3] for heavy ion scattering will be used at large separation. At short distances, we will parametrize the interaction potential by a set of Regge trajectories (or rotational bands) with two free parameters. The energy dependence of the imaginary interaction potential will be characterized by one free parameter. With these three parameters, we will analyze the gross oscillations of the excitation functions.

The organization of this paper is as follows. In Sec. II we will briefly discuss the DWBA and the Austern-Blair model. The diffraction model of Phillips *et al.* is analyzed in Sec. III A. The interference mechanism between the internal and barrier waves is studied in Sec. III B, together with the results of our calculations. Conclusion and remarks are presented in Sec. IV.

II. THE DISTORTED WAVE BORN APPROXIMATION AND THE AUSTERN-BLAIR MODEL

We consider the direct inelastic scattering to the low lying collective states. i.e., $A_1(0^+)+B_i(0^+)\rightarrow A_f(0^+)+B_f(J^\pi)$. The distorted wave transition amplitudes T_{fi} for the excitation of the target nucleus from the 0^+ state to the J^π state is given by

$$T_{fi}=(2J+1)^{1/2}A_J\beta^{JM}(\theta)\ , \tag{1}$$

where

$$\beta^{JM}(\theta)=\sum_{l_i l_f} i^{l_i-l_f-J}e^{i\sigma_{l_i}+i\sigma_{l_f}}(2l_f+1)^{1/2}I^{(J)}_{l_f l_i}\langle l_f 0\ J0\,|\,l_i 0\rangle\langle l_f -M\ JM\,|\,l_i 0\rangle Y^{-M}_{l_f}(\theta,0) \tag{2}$$

and A_J is the sepctroscopic factor for the transition of the nucleus from the $|0^+\rangle\rightarrow|J\pi\rangle$ state. In the above we defined $\hat{z}=\hat{k}_i$, $\hat{y}\propto\hat{k}_i x\hat{k}_f$, and θ as the scattering angle. The radial integral $I^{(J)}_{l_f l_i}$ is given by

$$I^{(J)}_{l_f l_i}=\frac{4\pi}{k_i k_f}\int_0^\infty dr\, f^{(f)}_{l_f}(k_f,r)F_J(r)f^{(i)}_{l_i}(k_i,r)\ , \tag{3}$$

where $f^{(f)}_{l_f}(r)$ and $f^{(i)}_{l_i}(r)$ are the radial parts of the distorted wave in the final and initial channels, respectively and the radial form factor $F_J(r)$ is defined via the transition amplitude

$$\langle\psi_{B_f}(J)\phi_{A_f}(0^+)\,|\,V_T\,|\,\psi_{B_i}(0^+)\phi_{A_i}(0^+)\rangle = \sum_J i^{-J}A_J F_J(r)Y^*_{JM}(\hat{r})\ . \tag{4}$$

In the collective model, the transition potential is given by

$$V_T(r)=R_0\frac{\partial U}{\partial R_0}\sum_{\lambda\mu}\alpha_{\lambda\mu}Y^*_{\lambda\mu}(\hat{r})+O(\alpha^2)\ . \tag{5}$$

The corresponding spectroscopic factor A_J and the radial form factor $F_J(r)$ are given by

$$A_J=i^J(2J+1)^{-1/2}\delta^{(N)}_J\ , \tag{6}$$

$$F_J(r)=\frac{\partial U}{\partial R_0}\ , \tag{7}$$

respectively, where $\delta^{(N)}_J$ is the deformation length, which can be determined from $A(e,e')$, $A(p,p')$ . . . experiments. The transition amplitude is given by

$$T^{\rm DW}_{JM}(\theta)=i^J\delta^{(N)}_J\beta_{JM}\ . \tag{8}$$

In the AB model, the radial integral $I^{(J)}_{l_f,l_i}$ is approximated by

$$I^{(J)}_{l_f l_i}\simeq\frac{i\pi\hbar^2}{\mu}\left[\frac{\partial\eta_f}{\partial\Lambda_f}\frac{\partial\eta_i}{\partial\Lambda_i}\right]^{1/2}\ , \tag{9}$$

where (η_f,Λ_f) and (η_i,Λ_i) are the S matrix and the grazing angular momentum of the final channel and initial channel, respectively. The AB model is usually misused with

$$I^{(J)}_{l_f l_i}\simeq-\frac{i\pi\hbar^2}{\mu}\left[\frac{\partial\eta_f}{\partial l_f}\frac{\partial\eta_i}{\partial l_i}\right]^{1/2}\ . \tag{10}$$

Equation (10) agrees with Eq. (9) in the strong absorption limit. For weak to moderate absorptive reactions, we should use Eq. (9) for the form factor. Therefore, in the present work, we use Eq. (9) in the analysis of the excitation functions. The validity of the AB model depends on the localization[9] of the angular momentum space for the radial integral $I^J_{l_f l_i}$. The localization is due to the phase averaging and absorption at low partial waves and small penetrability at high angular momentum. Because of large wave numbers and a moderate to strong absorption in the heavy ion scattering, the AB model should be quite reliable[9] in heavy ion scattering.

The angle integrated cross section is given by

$$\sigma_J=\frac{k_f}{4k_i}(2J+1)(\delta_J^{(N)})^2\sum_{l_f l_i}\hat{l}_f\hat{l}_i\begin{bmatrix} l_f & J & l_i \\ 0 & 0 & 0\end{bmatrix}^2 \times|\tilde{I}^{(J)}_{l_f l_i}|^2 , \tag{11}$$

where

$$\tilde{I}^{(J)}_{l_f l_i}\equiv\frac{\mu}{\pi\hbar^2}I^{(J)}_{l_f l_i} . \tag{12}$$

In the following section, we will analyze the energy dependence of the inelastic excitation function and study the effect of the molecular resonances on the gross oscillations in the excitation functions.

III. THE ANALYSIS OF EXCITATION FUNCTIONS

A. The diffraction model

The diffraction model is literally equivalent to the strong absorption model. The S matrix of the diffraction model can be expressed as the barrier wave S matrix in the semiclassical theory[8,10,11] of the potential scattering. The diffractive phenomenon in the heavy ion collision is related to the strong absorption for the low partial waves and the small penetrability for the large angular momentum. Therefore, the S matrix in the diffractive phenomenon of a potential is given by the barrier wave S matrix. At energies above the Coulomb barrier,[12] the semiclassical barrier wave S matrix can be approximated by the Ericson parametrization[13]

$$\eta_B(\lambda=l+\tfrac{1}{2})\cong\eta_{\text{Ericson}}=\frac{1}{1+e^{-i\gamma-(\lambda-\Lambda)/\Delta}} , \tag{13}$$

where Λ, Δ, and γ are the grazing angular momentum, the angular momentum diffuseness parameter, and the nuclear phase shift, respectively. The condition of the unitarity requires $|\gamma|\leq\pi/2$. Semiclassical analysis[8,10] of the heavy ion optical model potential shows that $\Delta\simeq(1/\pi)\,[(R_s/a)(1+V_C/2E)]^{1/2}$ for moderate to strong absorption and $\Delta\propto ka_w$ for a very strong absorption and at high energy. R_s, a, V_C, and E are, respectively, the strong absorption radius, the diffuseness parameter for the real potential, the Coulomb potential evaluated at $r=R_s$, and the center of mass energy. k and a_W are the wave number and the diffuseness parameter for the imaginary potential, respectively. The Ericson parametrization has poles in the first and fourth quadrants in the complex l plane. These poles are useful in simulating the diffractive phenomenon at energies higher than the Coulomb barrier.[10,12,14] The grazing angular momentum depends essentially only on the tail of the nuclear potential because of the large Coulomb and centrifugal barrier in the heavy ion collision. We choose the proximity type potential[3,15] for the ion-ion interaction at large distances, i.e.,

$$V(s)=-V_0\frac{R_1R_2}{R_1+R_2}e^{-s/a} , \tag{14}$$

where R_1 and R_2 are the radii of two ions, a is the diffuseness parameter, and s is the distance between the surfaces of two ions, $s=r-R_1-R_2$. The grazing angular momenta of the entrance and exit channels, Λ_i and Λ_f, can be evaluated by the incoming wave boundary condition model, i.e.,

$$\Lambda_{i,f}=k_{i,f}R_{i,f}\left\{\left[1-\frac{V_C(R_{i,f})}{E_{i,f}}\left[1-\frac{a}{R_{i,f}}\right]\right]\Big/\left[1-\frac{2a}{R_{i,f}}\right]\right\}^{1/2} . \tag{15}$$

The internal wave amplitude in the incoming wave boundary condition model is completely absorbed. Therefore, the elastic S matrix satisfying the incoming wave boundary condition is given by the barrier wave S matrix. The transition form factor in the AB model becomes

$$\tilde{I}^{B}_{l_{f_1} l_i} = -i \frac{1}{4(\Delta_f \Delta_i)^{1/2} \cosh\left[\frac{\lambda_f - \Lambda_f}{2\Delta_f} + i\frac{\gamma_f}{2}\right] \cosh\left[\frac{\lambda_i - \Lambda_i}{2\Delta_i} + i\frac{\gamma_i}{2}\right]} . \tag{16}$$

For low-lying state inelastic transitions, we expect that the ion-ion interaction potential is the same for the entrance and exit channels. Therefore, we take $\Delta_f = \Delta_i = \Delta$, $\gamma_f = \gamma_i = \gamma$, and Λ_f and Λ_i are calculated from the prescription we discussed in the previous paragraph, Eq. (15). The parameters of the potential are taken to be $V_0 = 24$ MeV/fm, $a = 0.68$ fm, and $R = R_1 + R_2 = 1.25(A_1^{1/3} + A_2^{1/3})$ fm. These parameters are chosen to give a reasonable grazing angular momenta for the heavy ion systems.

Figure 1 compares the experimental integrated cross section for the $^{12}C + ^{12}C \rightarrow ^{12}C + ^{12}C^*(2^+, 4.44$ MeV) reaction with the cross sections calculated with different Δ parameters. The calculated cross section is then normalized to 130 mb at $E = 30$ MeV. Our result has shown that (1) the Δ parameter must be around $0.8\hbar$ in order to account for the gross oscillation in the experimental cross section, and (2) at low energies, $E_{\text{c.m.}} < 20$ MeV, the experimental inelastic cross section is much larger than the barrier wave cross section. The Δ parameter in the Ericson parametrization is most sensitive to the diffuseness parameter a of the ion-ion interaction potential in Eq. (14). The Δ parameter, calculated from the optical potential, which fits the elastic

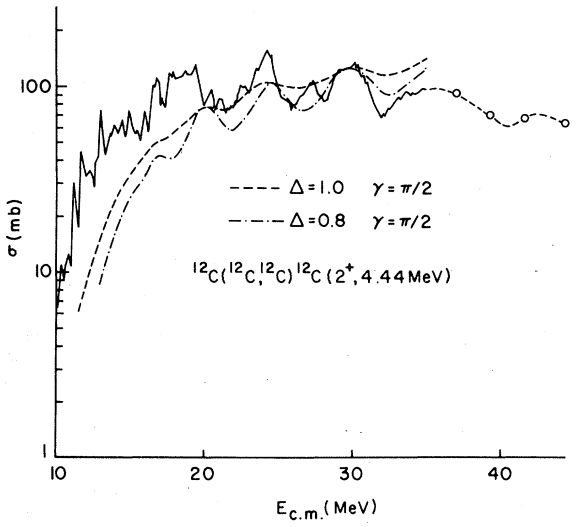

FIG. 1 The experimental excitation function (solid) is compared with that calculated from the diffraction model. The Ericson parametrization is used to represent the barrier wave S matrix of the diffraction model.

scattering of heavy ion collision, has a value normally larger than $1.0\hbar$. It is almost impossible to obtain a Δ parameter around $0.8\hbar$ in any standard optical model calculation. This is because the diffuseness parameter and the nuclear radius are known to have an error of less than 30%. Thus, the small angular momentum window used by the diffraction model serves only to mock up the gross oscillation in the excitation function. The kinematic matching condition emphasized by the diffraction model cannot be the essential mechanism of the oscillatory behavior in the excitation function. Besides, the angular momentum window must be smaller than $0.4\hbar$ in order to give a gross oscillatory behavior in the total reaction cross section.

It is known that the diffractive scattering process does exhibit an oscillatory angular distribution and an oscillatory fixed-angle excitation function. This oscillatory feature has been attributed to the interference effect of far-side and near-side rays of the surface waves.[12–14] It is, however, incorrect to associate the oscillatory structure of the angle-integrated excitation function to the interference effect in the diffraction model. This point of view is trivial from Eq. (11) that the cross section is an incoherent sum of the radial integrals $\tilde{I}^{(J)}_{l_f l}$, which is a smooth function of l_f and l_i in the diffraction model. Thus, the interference effect must exhibit itself in each term of I_{l_f, l_i}, i.e., interference between the internal and barrier waves. We therefore conclude that the internal wave contribution and the resonances of the heavy ion system must be very important in understanding the gross oscillation in the excitation functions.

B. The internal wave S matrix and the molecular resonance of the heavy ion system

The internal wave S matrix describes the scattering process that the incident wave enters the interior potential well and reemits. At the potential resonance, which is defined as the standing wave inside the potential well, the internal wave undergoes multiple reflections and at the same time the internal wave also interferes destructively with the barrier wave component.[8] As the strength of the imaginary potential increases, the effect of the multiple reflections within the potential well diminishes.

Yet the interference between the barrier and internal waves remains as the indicator of the potential resonance.[8] Most of the heavy ion optical potentials, which fit the elastic scattering data have moderate to strong absorptions. Therefore, the effect of the multiple reflections is not important. The resonance exhibits itself essentially through the interference phenomenon. In this section, we will study the internal wave S matrix with overlapping resonances and their interference with the barrier wave component. We will not discuss in this paper the possible l or J dependence[7] or the surface transparency in the imaginary part of the optical potential.

The internal wave S matrix for a moderate absorptive heavy ion optical potential can be expressed as [11]

$$\eta_I(\lambda)=|\eta_I(0)|\frac{e^{2i\delta_I(\lambda)}}{1+e^{i\gamma_I+(\lambda-\Lambda)/\Delta_I}}, \tag{17}$$

where Λ, Δ_I, and γ_I are the grazing angular momentum, the angular momentum diffuseness, and the nuclear phase shift near the surface. The grazing angular momentum is the same as that of the barrier wave. The angular momentum diffuseness Δ_I for the internal wave S matrix is about half that of the barrier wave S matrix,[11] i.e., $\Delta_I \simeq \Delta/2$. $\delta_I(\lambda)$ is the phase shift of the internal wave S matrix.

The transition radial integral in the AB model is given by

$$|\tilde{I}_{l_f l_i}|^2=|\tilde{I}^B_{l_f l_i}|^2\left|\left[1-2|\eta_I(0)|\frac{\cosh\left[\frac{\lambda_f-\Lambda_f}{\Delta}\right]+\cos\gamma_B}{\cosh\left[2\frac{\lambda_f-\Lambda_f}{\Delta}\right]+\cos\gamma_I}\exp\{2i[\delta^I(\lambda_f)-\delta^B(\lambda_f)+\phi_f]\}\right]\right.$$
$$\left.\times\left[1-2|\eta_I(0)|\frac{\cosh\left[\frac{\lambda_i-\Lambda_i}{\Delta}\right]+\cos\gamma_B}{\cosh\left[2\frac{\lambda_i-\Lambda_i}{\Delta}\right]+\cos\gamma_I}\exp\{2i[\delta^I(\lambda_i)-\delta^B(\lambda_i)+\phi_i]\}\right]\right|, \tag{18}$$

with

$$\phi_i=\tan^{-1}\frac{\sinh\frac{\lambda_i-\Lambda_i}{2\Delta}\sin\frac{\gamma_B}{2}}{\cosh\frac{\lambda_i-\Lambda_i}{2\Delta}\cos\frac{\gamma_B}{2}}-\tan^{-1}\frac{\sinh\frac{\lambda_i-\Lambda_i}{\Delta}\sin\frac{\gamma_I}{2}}{\cosh\frac{\lambda_i-\Lambda_i}{\Delta}\cos\frac{\gamma_I}{2}}. \tag{19}$$

$\tilde{I}^B_{l_f l_i}$ is the barrier contribution [Eq. (16)], and $2\delta^I(\lambda)$ and $2\delta^B(\lambda)$ are the internal wave and the barrier wave phase shifts for angular momentum $\lambda=l+\frac{1}{2}$, respectively.

If the heavy ion optical potential is deep, e.g., the real depth $V_0 \geq 100$ MeV, we can show that[8,10]

$$2\delta^I(\lambda)-2\delta^B(\lambda)\cong 2\delta_0(E)-l\pi. \tag{20}$$

The phase shift $2\delta_0(E)$ depends only on the interaction between two ions at short distances. We can parametrize the phase shift as

$$\delta_0(E)=C_1+C_2E. \tag{21}$$

This parametrization is equivalent to having a linear Regge resonance trajectory for the composite heavy ion system, i.e.,

$$l_n(E)=-2n-1+2C_1/\pi+(2C_2/\pi)E. \tag{22}$$

The linear trajectory should be a fair approximation to the band of the molecular resonances of the composite heavy ion system in a limited energy range of interest, e.g., 20 MeV $\leq E_{\text{c.m.}} \leq$ 40 MeV. By allowing a slow energy dependence of the c_2 parameter, the parametrized Regge trajectory [Eq. (22)] can also simulate the rotational band of the molecular resonances. The energy spacing of these molecular resonances is given by $\pi/2$ $[2C_2+2E(dC_2/dE)]$.

The energy dependence of the internal wave amplitude, $|\eta_I(0)|$, and the energy dependence of the imaginary potential are related by $|\eta_I(0)| = e^{-W_0(E)\tau_i}$, derived from the semiclassical analysis of the optical potentials.[8] We therefore use

$$|\eta_I(0)| = e^{-C_3 E} \tag{23}$$

to represent the phenomenological linear dependence of the imaginary strength on the energy. We set $\gamma_B = \gamma_I = \pi/2$ to be independent of the energy. This is because the magnitude of the integrated cross section does not depend sensitively on the phase γ_B and γ_I, and besides, γ_B and γ_I depend slowly on the energy.[11]

We have therefore only three parameters, C_1, C_2, and C_3, in our model to fit the data. The grazing angular momenta Λ_i and Λ_f are calculated from the incoming wave boundary condition model with the proximity potential in Eq. (15). The parameter $\Delta = 1.0$ is used. Using $\Delta = 1.0 \sim 1.3$ does not change the analysis dramatically. Figure 2 shows the experimental $2^+(4.44$ MeV) inelastic excitation function of the $^{12}C + ^{12}C$ system and the calculated excitation of this model. The parameters C_1, C_2, and C_3 are adjusted to fit the data. We obtain $C_1 = 0.2$, $C_2 \simeq 0.57$/MeV, and $C_3 = 0.085$/MeV. The $C_2(E)$ as a function of energy is shown in Fig. 3.

The total reaction cross section is given by

$$\begin{aligned}\sigma_R &= \frac{\pi}{k^2}\sum_l (2l+1)(1-|\eta_l|^2) \\ &= \frac{\pi}{k^2}\sum_l (2l+1)(1-|\eta_l^B|^2) - \frac{\pi}{k^2}\sum_l (2l+1)|\eta_l^I|^2 \\ &\quad -2\frac{\pi}{k^2}\sum_l (2l+1)|\eta_l^I \eta_l^B| \cos\left[2\delta_I(l) - 2\delta_B(l) + \frac{\gamma_I+\gamma_B}{2} + \phi\right] .\end{aligned} \tag{24}$$

In Fig. 2, we also compare the calculated total reaction cross section with the experimental fusion cross section.[16] The fusion cross section should be equal to the total reaction cross section minus the total direct reaction cross sections. From Fig. 2, we observe that the oscillations of the fusion cross section match quite well with that of the total reaction cross section. When the entrance grazing angular momentum Λ_i passes through a resonance, $2\delta_I(\Lambda_i) - 2\delta_B(\Lambda_i) + (\gamma_I+\gamma_B)/2 + \phi_i = 2(n+\frac{1}{2})\pi$, the reaction cross section is at maximum. This is related to the fact that the wave function is well matched at the resonance and is pulled into the nuclear interior to give rise to a large reaction cross section.

By comparing Figs. 1 and 2, we find that the low lying state inelastic excitation function can be fitted by the diffraction model or by the interference mechanism between the internal and barrier waves. In the diffraction model, one has to use a very small angular momentum window, $\Delta \leq 0.8\hbar$, in order to simulate the effect of the kinematical matching condition for the reaction. The parameter $\Delta \leq 0.8\hbar$ is, unfortunately, inconsistent with that obtained from the standard optical potentials. As a second explanation, one emphasizes the collective effect of the overlapping resonances to the phase shift and the interference of the internal wave with the barrier wave S matrices. The gross oscillation in the inelastic excitation function is due essentially to the resonance interference mechanism but not to the kinematic angular momentum matching condition.

Figure 4 shows the similar fit to the $^{16}O + ^{16}O \rightarrow ^{16}O + ^{16}O^*(3^-, 6.13$ MeV) inelastic excitations function.[17] We obtain $C_1 = -0.2$, $C_2 \cong 0.78$/MeV, and $C_3 = 0.085$/MeV. The energy dependence of $C_2(E)$ is shown with the Regge slopes of the $^{16}O + ^{16}O$ system. The Regge poles of the $^{16}O + ^{16}O$ systems are taken from the calculation by Tamura and Walter[18] for the optical potentials which fit the $^{16}O + ^{16}O$ system.[7,19] The slope of the solid line, drawing through the □ and Δ, is 1.35/MeV in the energy range 20 MeV $\leq E \leq$ 45 MeV. This is in good agreement with that of our analysis, $2C + 2E(dC_2/dE) = 1.31$/MeV at $E = 32$ MeV. Figure 5 also shows the Regge trajectories of the $\alpha + ^{40}$Ca system, which are taken from the semiclassical analysis[10] of the optical potential of Michel and Vanderpoorten.[20] The Regge slope in our analysis is undoubtedly related to the moment of inertia of the composite system.

C. Discussion

Our results show that the molecular resonance plays an important role in the heavy ion excitation

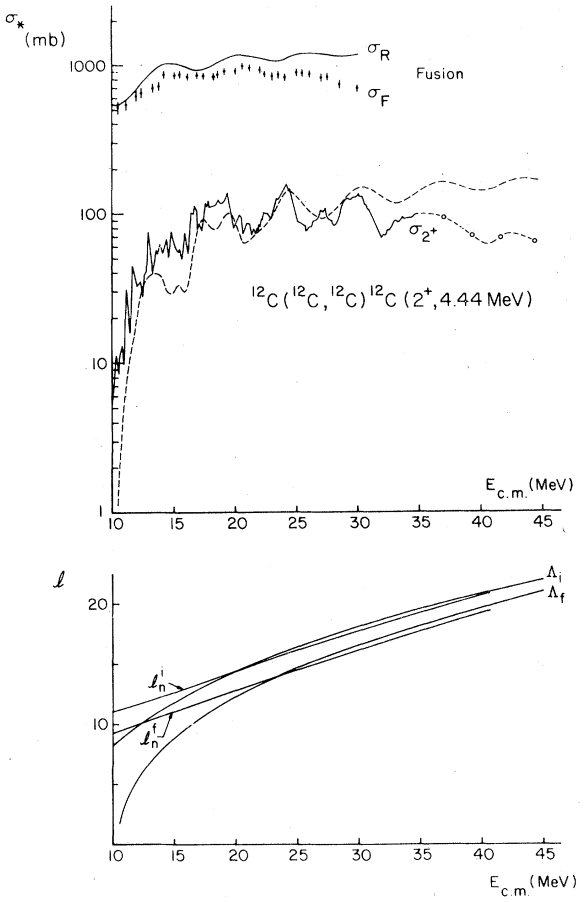

FIG. 2. The inelastic excitation function for the $^{12}C+^{12}C$ system (dashed line) calculated with the interference effect between the internal and barrier wave amplitudes is compared with the experimental excitation function (solid line). The calculated cross sections are normalized with a deformation length $\delta_2^{(N)}=1.00$ fm, which is equivalent to a deformation parameter $\beta\simeq 0.2$. In the upper part of the figure, the fusion cross section (see Ref. 16) is compared with the calculated total reaction cross section. The grazing angular momenta and the important Regge trajectories of the entrance and exit channels are also shown in the lower part of the figure.

functions. The peak energy of the total reaction cross section and the fusion cross section may be associated with the entrance channel resonances at the grazing angular momentum, i.e., when

$$2\delta_I(\Lambda_i)-2\delta_B(\Lambda_i)+\frac{\gamma_I+\gamma_B}{2}+\phi_i(\Lambda_i)$$
$$=2(n+\tfrac{1}{2})\pi \qquad (25)$$

happen at an integer grazing angular momentum $L_i=\Lambda_i-\frac{1}{2}$, the total reaction cross section has a

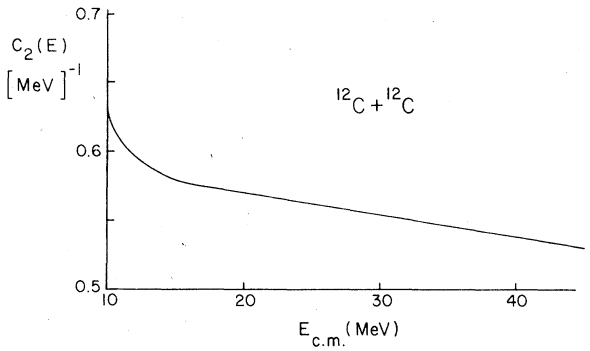

FIG. 3. The energy dependence of the C_2 parameter of the Regge slope.

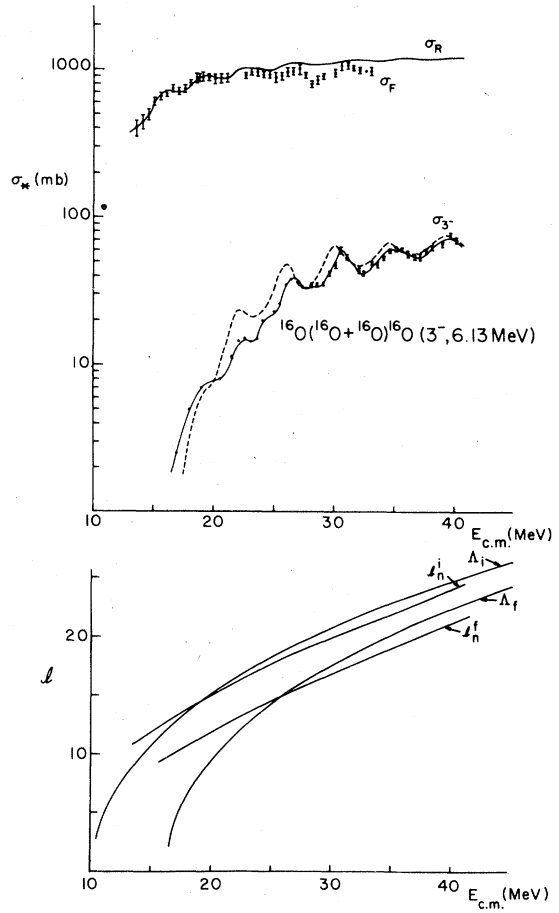

FIG. 4. Experimental inelastic and fusion excitation functions of the $^{16}O+^{16}O$ system are compared with the calculated excitation functions. See caption of Fig. 2 for each curve. The deformation parameter $\delta=1.12$ fm for the ^{16}O (3^-) state is obtained. The data is taken from Ref. 17.

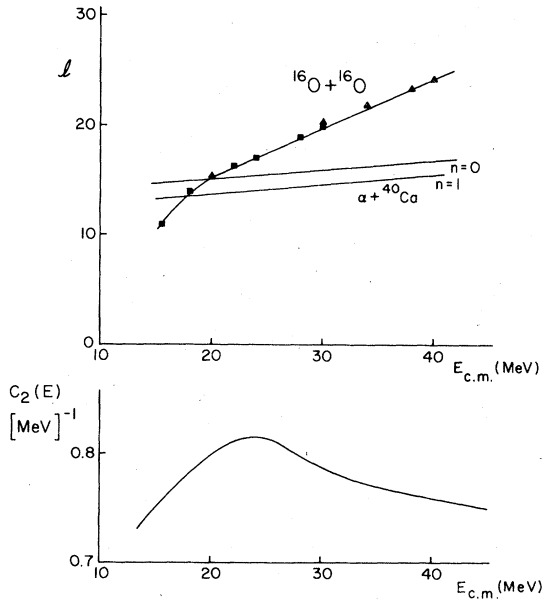

FIG. 5. The energy dependence of the $C_2(E)$ and the Regge trajectories of the $^{16}O+^{16}O$ and $\alpha+^{40}Ca$ systems are shown for comparison.

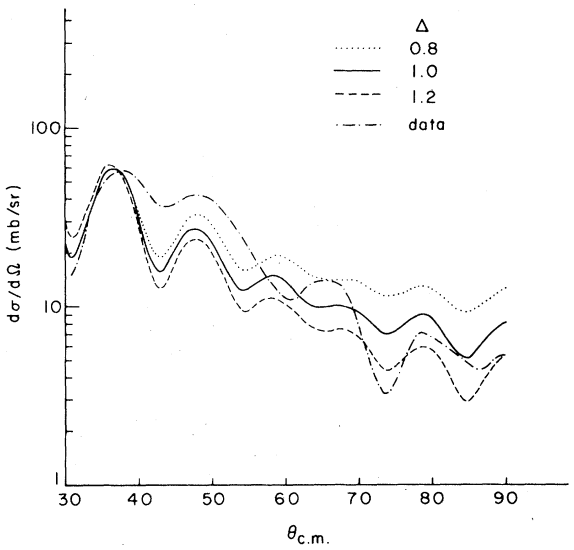

FIG. 6. Experimental angular distribution (Ref. 21) of $^{12}C+^{12}C\rightarrow^{12}C+^{12}C(2^+, 4.44$ MeV) is compared with that of the diffraction model ($=0.8\hbar$) and that of the interference model ($\Delta=1.0\hbar$ and $\Delta=1.2\hbar$).

peak. On the other hand, when the exit as well as the entrance channel phase shifts satisfy the relation

$$2\delta_I(\lambda)-2\delta_B(\lambda)+2\phi_{i,f}(\lambda) = 2(n+\tfrac{1}{2})\pi\,, \tag{26}$$

at the exit or entrance channel angular momentum $l=\lambda-\frac{1}{2}$ around the grazing angular momenta, the inelastic excitation function has a peak. The correlation of the peak positions in the excitation function of the total reaction and the integrated inelastic cross sections is clear from Eqs. (25) and (26). The angular momentum matching condition does not give rise to a dynamical origin of these gross oscillations in the excitation functions. To investigate the implication of a small angular momentum window Δ parameter, we calculate the angular distribution of the $^{12}C+^{12}C\rightarrow^{12}C+^{12}C(2^+, 4.44$ MeV) at $E_{c.m.}=25$ MeV. Figure 6 shows the differential cross sections with $\Delta=0.8\hbar$, $1.0\hbar$, and $1.2\hbar$, respectively. It is clearly seen that the Δ parameter must be larger than $1.0\hbar$ in order to be consistent with the slope of the angular distribution.

Our analysis is based on the DWBA. The result indicates that these molecular resonances are overlapping. At energy $E>20$ MeV, $|\eta_I|\leq 0.18$. Therefore, the multiple reflection (MR) in the internal wave amplitude is not important.[8] Thus, the DWBA should be a good approximation. The corresponding damping width $\Gamma^{\downarrow}\cong 2W_0$ at $E=20$ MeV would be about 2.5 MeV, which is estimated[8] from $|\eta_I(0)|\simeq e^{-W_0\tau_t}$. The elastic width can be estimated from the Wigner limit, i.e.,

$$\Gamma_J^{\uparrow}\simeq 3\frac{\hbar^2}{MR^2}P_J(E)\leq\frac{3\pi}{4C_2J}\,, \tag{27}$$

where we have used $\Delta E\simeq\hbar^2/MR^2 2J\simeq\pi/2C_2$. The escape width $\Gamma_J^{\uparrow}$ is typically only of the order of 0.2 MeV at the grazing angular momentum for $^{12}C+^{12}C$ and $^{16}O+^{16}O$ systems in our study. We observe, therefore, that these resonances have a relatively small partial width to the elastic and direct reaction channels. The major part of the width goes to the absorption $\Gamma^{\downarrow}$. Therefore, the terminology of molecular resonance may be inappropriate, yet the elastic width can still be the largest partial width in Γ_{tot}. Our analysis shows that the deformation length extracted from the data is not very large and is therefore consistent with the DWBA treatment. The partial width to these low lying collective states must be also small. These overlapping resonances, yet, show up themselves in the interference mechanism of the barrier and internal waves.

At energy $E<20$ MeV, the $^{12}C+^{12}C$ data have many interesting fine structures. The multiple re-

flections in our analysis become important at energy $E < 20$ MeV. The coupled channel effect is important. Experimental and theoretical investigations at these energy ranges will be fruitful in pinning down the detailed physics of the fine structures. These fine structures are beyond the scope of the present investigation.

IV. CONCLUSION AND REMARKS

We have investigated the physical implication of the diffraction model interpretation to the angle-integrated inelastic excitation function for low-lying collective states. We find that the model requires a very small angular momentum window, i.e., $\Delta \lesssim 0.80\hbar$, in order to account for the gross oscillation in the experimental data. The heavy ion proximity potential at large separation, however, predicts a much larger angular momentum diffuseness, $\Delta \gtrsim 1.0\hbar$. This discrepancy implies that either the model is inadequate or we have to abandon the concept of the heavy ion interaction potential. We do know, through many elastic scattering data, that the interaction potential between ions at large separation is not very much different from the proximity potential. We therefore believe that the diffraction model is inadequate and serves only to mock up the gross oscillation in the excitation function.

On the other hand, we have shown that the gross oscillation in the excitation function can easily be explained by the interference mechanism between the barrier and internal wave S matrices. The interference between the barrier and internal wave amplitudes is a manifestation of the existence of the potential resonances. We have assumed a set of Regge trajectories for the heavy ion interaction. The direct surface reaction probes only the resonances near the grazing angular momentum. When the resonances overlap with each other, the effect of multiple reflection is not important. In this case, the wave function is pulled into the nuclear interior at the resonance due to a good matching condition at the barrier. Thus, the total reaction (and probably the fusion) cross section is at maximum. On the other hand, the wave function at the surface region is modulated by a phase shift at the surface region of the interaction potential; we reach a small energy shift in the gross oscillation of the inelastic excitation function. The correlation between the fusion and the direct surface reaction excitation functions (see Figs. 2 and 4) gives strong support to our model.

ACKNOWLEDGMENTS

The authors thank Professor P. Braun-Munzinger, G. E. Brown, and Professor P. Paul for helpful discussions and encouragement. We also thank Professor K. A. Erb for a helpful correspondence. This work was supported in part by the U. S. Department of Energy under Contract No. DE-AC02-T6ER13001.

[1]R. L. Phillips, K. A. Erb, D. A. Bromley, and J. Weneser, Phys. Rev. Lett. 42, 566 (1979).

[2]T. M. Cormier *et al.*, Phys. Rev. Lett. 40, 924 (1978); 38, 940 (1978); H. Emling *et al.*, Nucl. Phys. A211, 600 (1973); R. Wieland *et al.*, Phys. Rev. C 8, 37 (1973); B. R. Fulton *et al.*, Univ. of Rochester Report UR-NSRL-22.

[3]J. Blocki, J. Randrup, W. J. Swiatecki, and C. F. Tsang, Ann. Phys. (N. Y.) 105, 427 (1977); H. J. Krappe, J. R. Nix, and A. J. Sierk, Phys. Rev. Lett. 42, 215 (1979).

[4]W. A. Friedman, K. W. McVoy, and M. C. Nemes, Phys. Lett. 87B, 179 (1979).

[5]W. A. Friedman and C. J. Goebel, Ann. Phys. (N. Y.) 104, 145 (1977).

[6]Y. Kondo and T. Matsuse, Prog. Theor. Phys. 59, 1393 (1978); O, Tanimura and T. Tazawa, Phys. Lett. 83B, 22 (1979); Phys. Rev. C 20, 183 (1979); Phys. Rep. 61, 255 (1980); B. Imanishi, Phys. Lett. 27B, 267 (1968); Nucl. Phys. A274, 177 (1976).

[7]R. A. Chatwin, J. S. Eck, A. Richter, and D. Robson Phys. Rev. 180, 1049 (1969); Phys. Rev. C 1, 795 (1970).

[8]D. M. Brink and N. Takigawa, Nucl. Phys. A279, 159 (1977); S.Y. Lee, N. Takigawa, and C. Marty, *ibid.* A308, 161 (1978).

[9]N. Austern and J. S. Blair, Ann, Phys, (N. Y.) 33, 15 (1965); F. J. W. Hahne, Nucl. Phys. A104, 545 (1967); A106, 660 (1968).

[10]N. Takigawa and S. Y. Lee, Nucl. Phys. A292, 173 (1977).

[11]S. Y. Lee, Nucl. Phys. A311, 518 (1978).

[12]R. C Fuller, Phys. Rev. C 12, 1561 (1977); R. C. Fuller and P. J. Moffa, *ibid.* 15, 266 (1977).

[13]T. E. O. Ericson, *Preludes in Theoretical Physics,* edited by A. de-Shalit, H. Feshbach, and L. Van Hove

(North-Holland, Amsterdam, 1966), p. 321.
[14]N. Rowley and C. Marty, Nucl. Phys. A266, 494 (1977).
[15]P. R. Christian and A. Winther, Phys. Lett. 65B, 19 (1976).
[16]P. Sperr, T. H. Braid, Y. Eisen, D. G. Kovar, F. M. Prosser, Jr., J. P. Schiffer, S. L. Tabor, and S. Vigdor, Phys. Rev. Lett. 37, 321 (1976).
[17]J. J. Kolata, R. C. Fuller, R. M. Freeman, F. Haas, B. Heusch, and A. Gallmann, Phys. Rev. C 16, 891 (1977); J. J. Kolata, R. M. Freeman, F. Haas, B. Heusch and A. Gallmann, *ibid.* 19, 2237 (1979).
[18]T. Tamura and H. H. Walter, Phys. Rev. C 6, 1976 (1972).
[19]J. V. Maher, M. W. Sachs, R. H. Siemssen, A. Weidinger, and D. A. Bromley, Phys. Rev. 188, 1665 (1969).
[20]F. Michel and R. Vanderpoorten, Phys. Rev. C 16, 142 (1977).
[21]R. Wieland, Ph.D. dissertation Yale University, 1973 (unpublished).